



ELSEVIER

Available online at www.sciencedirect.com

ScienceDirect

journal homepage: www.elsevier.com/locate/ijhydene

An in-situ DRIFTS-MS study of the photocatalytic H₂ production from ethanol_(aq) vapour over Pt/TiO₂ and Pt–Ga/TiO₂ catalysts

Alberto C. Sola ^{a,b}, Narcís Homs ^{a,b}, Pilar Ramírez de la Piscina ^{a,*}

^a *Departament de Química Inorgànica i Orgànica, Secció de Química Inorgànica and Institut de Nanociència i Nanotecnologia (IN2UB), Universitat de Barcelona, Martí i Franquès 1-11, 08028, Barcelona, Spain*

^b *Insitut de Recerca en Energia de Catalunya (IREC), Jardins de les Dones de Negre 1, 08930, Barcelona, Spain*

ARTICLE INFO

Article history:

Received 15 September 2017

Received in revised form

6 February 2018

Accepted 15 February 2018

Available online xxx

Keywords:

H₂ photoproduction

Renewable H₂

Pt–Ga/TiO₂ photocatalyst

In-situ DRIFTS

Photocatalytic H₂

Ethanol photoconversion

ABSTRACT

In this paper, Pt/TiO₂ and Pt–Ga/TiO₂ catalysts with similar Pt dispersion and similar structural and morphological characteristics were compared in the H₂ production from the phototransformation of aqueous solutions of ethanol. Catalysts were characterized by means of N₂ adsorption-desorption, XRD, Raman, H₂-TPR, UV–Vis diffuse reflectance spectroscopy, XPS and CO chemisorption. The photocatalytic reaction was carried out in liquid and vapour phase. The photocatalytic transformation of ethanol_(aq) vapour over Pt/TiO₂ and Pt–Ga/TiO₂ catalysts was studied by in situ DRIFTS-MS. Differences in the photocatalytic transformation of ethanol_(aq) over Pt/TiO₂ and Pt–Ga/TiO₂ were determined. The effect of Ga is analysed in the light of the evolution of surface species under photocatalytic reaction conditions.

© 2018 Hydrogen Energy Publications LLC. Published by Elsevier Ltd. All rights reserved.

Introduction

Since pioneer work of Sakata and Kawai [1], numerous studies have dealt with the photocatalytic hydrogen production using a metal-modified TiO₂ photocatalyst and ethanol-water solutions [2–7]. In particular, the photocatalytic production of H₂ from aqueous ethanol solutions over Pt/TiO₂ has been widely studied [8–12]. Ethanol, which is the sacrificial agent, is oxidized by photogenerated holes in TiO₂ and H₂ is produced by H⁺ reduction at the surface of Pt nanoparticles [13,14]. The final product of ethanol oxidation would be CO₂ if the process is totally completed. However, ethanol oxidation takes place in

several consecutive steps; intermediate products such as acetaldehyde and acetic acid are usually found in the solution when the reaction takes place in liquid phase [14–16]. If the photocatalytic process is carried out in a semi-batch reactor, in which the liquid products are not removed, the intermediate products formed could compete with ethanol for the adsorption sites and this could affect the rate of H₂ production over the reaction time. In this context, we have recently shown that using a Pt/anatase photocatalyst the irradiation of ethanol_(aq) resulted in higher rates of hydrogen production than those obtained from acetaldehyde or acetic acid solutions [12].

There are many works in which the effect of dopants in the photocatalytic behaviour of TiO₂ has been studied [11,17,18].

* Corresponding author.

E-mail address: pilar.piscina@qi.ub.es (P. Ramírez de la Piscina).

<https://doi.org/10.1016/j.ijhydene.2018.02.098>

0360-3199/© 2018 Hydrogen Energy Publications LLC. Published by Elsevier Ltd. All rights reserved.

However, when dopants are introduced in Pt/TiO₂-based catalysts, they can also influence the characteristics of Pt nanoparticles producing a change in the photocatalytic behaviour of the initial Pt/TiO₂.

We have recently reported the promoter effect of Ga related with the modification of surface Pt species. Pt–Ga/TiO₂ catalysts containing about 0.5% wt Pt and small amounts of Ga (0.2–0.6% wt) showed higher Pt dispersion values and lower relative amount of surface oxidized Pt species than related Pt/TiO₂ (0.5% wt Pt). In this initial work, the photocatalytic conversion of ethanol_(aq) was studied in liquid phase and the behaviour of Pt–Ga/TiO₂ catalysts was compared to that of a Pt/TiO₂ catalyst having similar Pt content but much lower Pt dispersion [19].

For a better insight of the effect of Ga on the photocatalytic behaviour of Pt/TiO₂ catalysts, here we report an *in-situ* DRIFTS-MS study of the photocatalytic transformation of ethanol/H₂O vapour mixtures over a Pt–Ga/TiO₂ catalyst. The surface species formed and their evolution during irradiation are compared with those formed when a Pt/TiO₂ catalyst with a similar Pt dispersion is used.

Experimental

Preparation and characterization of catalysts and catalytic tests in liquid phase

Pt/TiO₂ catalysts were prepared by incipient wetness impregnation using H₂PtCl₆·6H₂O aqueous solutions and anatase TiO₂ from Sigma Aldrich. After the impregnation, the catalysts were dried at 70 °C for 1 h and calcined at 400 °C for 4 h. A similar method was used for the preparation of Pt–Ga/TiO₂. In this case, Ga was previously impregnated using Ga(NO₃)₃·xH₂O as precursor and then, after drying and calcination, the resulting solid was used for Pt incorporation as described elsewhere [19].

Pt and Ga contents were determined by inductively-coupled plasma (ICP) atomic emission spectrometry using a Perkin Elmer Optima 3200RL.

The surface area (S_{BET}), pore volume (V_{pore}) and pore diameter (D_{pore}) of the photocatalysts were determined by N₂ adsorption-desorption isotherms at –196 °C using a Micromeritics TriStar II 3020 system.

H₂-TPR analysis and CO chemisorption experiments were performed using a Micromeritics Autochem II 2920 system. For the H₂-TPR experiments, a 10% (v/v) H₂/Ar flow and a heating rate of 10 °C min^{–1} were used. CO chemisorption was carried out at 35 °C. Before the CO chemisorption, the samples were reduced at 125 °C under a 10% (v/v) H₂/Ar stream for 45 min and then purged with He (30 min at 125 °C).

XRD analysis was done using an Xpert PRO-diffractometer equipped with a CuK α radiation source ($\lambda = 1.5406 \text{ \AA}$) and a graphite monochromator. The XRD patterns were collected between $2\theta = 10^\circ$ and $2\theta = 100^\circ$, with a step width of 0.05°, counting 3 s at each step. The Scherrer equation was used for the estimation of the mean TiO₂ crystallite size.

UV–Vis diffuse reflectance spectroscopy was used for the determination of the band-gap values. The spectra were registered using a Perkin Elmer Lambda 950 UV/Vis

Spectrometer with a 3 nm slit width and a speed of 654.92 nm min^{–1}; BaSO₄ was used as the reference. The reflectance was converted into the equivalent absorption coefficient, $F(R_{\infty})$, using the Kubelka-Munk formalism. The band-gap values were calculated using the Tauc plot, $(F(R_{\infty}) \cdot h\nu)^n$ versus $h\nu$, where $n = 1/2$ indicates an indirect allowed transition [20].

A Perkin Elmer PHI-5500 spectrometer equipped with an Al K α source (1486.6 eV) and a hemispherical analyser was used to perform the X-ray photoemission spectra. The pressure in the analysis chamber was maintained below 10^{–8} torr during data acquisition. The adventitious C 1 s peak at 284.8 eV was used as reference for the determination of binding energy (BE) values.

The experimental setup used for carried out the catalytic tests in liquid phase has been described elsewhere [12,19]. In short, photocatalytic experiments were carried out at 25 °C using a semi-batch reactor equipped with inlet and outlet opening for gases and a 175 W Hg lamp (broad spectrum lamp, maximum power at $\lambda = 366 \text{ nm}$: 25.6 W); the lamp was placed in a water-cooled quartz jacket inside the reactor. For the photocatalytic test, 0.5 g of catalysts and 250 mL of an ethanol/water solution 25% (v/v) were used; the suspension was magnetically stirred and flushed with inert gas during the tests. The gaseous products were periodically sampled and analysed by gas chromatography. The liquid was analysed at the end of the test by gas chromatography and IR-ATR spectroscopy.

In situ DRIFTS-MS study

In situ DRIFTS experiments were carried out using a FTIR spectrophotometer Bruker Vertex 70 in DRIFT mode, coupled to a mass spectrometer ThermoStar GSD320T1. The samples were deposited into a reaction chamber and irradiated with a Hamamatsu Lightning Cure lamp ($\lambda = 365 \text{ nm}$, 20 mW cm^{–2}). The samples were pre-treated at 150 °C under He flow for 30 min, and the background spectrum was registered at 25 °C. Then, a He flow saturated with ethanol/water vapour = 1/9.6 (mol/mol) was entered into the chamber at room temperature. After the adsorption, the ethanol/water flowing mixture was stopped and the catalysts were treated under He flow at room temperature until negligible evolution of reactants was detected by MS (about 15 min). Then, the initial DRIFT spectrum was recorded, and the catalyst was irradiated under He flow at 25 °C. During irradiation under He flow, DRIFT and mass spectra were recorded as a function of time (total time 50 min). DRIFT spectra were recorded at a resolution of 4 cm^{–1} and corrected with the adsorbed water spectrum. The m/z fragments corresponding to CH₃CH₂OH, CH₃CHO, CH₃COOH, CH₄, CO₂, CO and H₂ were analysed by MS.

Results and discussion

Characteristics of the catalysts and photocatalytic behaviour in liquid phase

Table 1 shows several characteristics of the photocatalysts studied in this work. Although all catalysts had similar values

Table 1 – Several characteristics of catalysts.

Catalysts	S_{BET} ($\text{m}^2 \text{g}^{-1}$)	V_{pore} ($\text{cm}^3 \text{g}^{-1}$)	D_{pore} (nm)	Band gap (eV)	Pt (%wt)	Ga (%wt)	Pt dispersion (%)	d_{Pt} (nm)	$\text{molH}_2/\text{molPt}^{\text{a}}$
0.3Pt/TiO ₂	56	0.27	29.1	3.18	0.27	–	70	1.6	2.9
0.4Pt/TiO ₂	56	0.27	29.1	3.18	0.38	–	68	1.7	2.5
Pt–Ga/TiO ₂ ^b	46	0.24	23.0	3.14	0.51	0.19	75	1.5	1.7

^a H₂ consumption from H₂-TPR experiments.

^b Results from [19].

of surface-area, pore volume and pore width, the values corresponding to 0.4Pt/TiO₂ and 0.3Pt/TiO₂ were slightly higher than those of Pt–Ga/TiO₂. XRD patterns (not shown) indicated in all cases the presence of anatase as the solely crystalline phase with an estimated size of 22 nm. According with XRD results, Raman spectra only revealed bands at ca. 639 cm⁻¹ (E_g), 515 cm⁻¹ (A_{1g} + B_{1g}), 399 cm⁻¹ (B_{1g}), 197 cm⁻¹ (E_g) and 144 cm⁻¹ (E_g), characteristic of anatase [21]. The band-gap values were slightly lower than that of the TiO₂ used in the preparation of catalysts (TiO₂ band gap: 3.23 eV). Catalysts containing only Pt showed somewhat higher band-gap than Pt–Ga/TiO₂ according with previous results [19].

In all cases, the analysis of calcined catalysts by XPS showed Pt 4f_{7/2} peaks centred at 72.2–72.6 eV, which were attributed to PtO_x surface species (Fig. 1). Ti 2p_{3/2} peaks centred at 458.7 eV and O 1s peaks with maximum at 529.9 eV were found and related to Ti⁴⁺ and surface oxide species, respectively [22].

H₂-TPR profiles (Fig. 2) pointed out differences in the reduction characteristics of the catalysts. For 0.4Pt/TiO₂ and 0.3Pt/TiO₂ the reduction peaks were clearly asymmetric and the corresponding H₂ consumption (Table 1) was higher than the theoretical if the reduction of PtO₂ is assumed (H₂/Pt = 2 mol/mol). This excessive H₂ consumption is associated with the partial reduction of TiO₂, which can be favoured by the H₂ adsorption onto Pt and the ulterior spill over effect on TiO₂. For Pt–Ga/TiO₂, the partial decomposition of PtO₂ during

the calcination forming PtO and/or Pt could justify the H₂/Pt < 2 (mol/mol) obtained [23].

In order to evaluate the Pt dispersion of the catalysts, CO chemisorption experiments were performed at 35 °C over the catalysts previously reduced at 125 °C. Using a stoichiometry of adsorption 1:1 (adsorbed CO molecule: surface Pt atom) and considering the presence of cubic Pt particles, both the dispersion and the Pt particle size were determined. Values of Pt dispersion in the range 68–75% and Pt particle size of 1.7–1.5 nm were obtained (Table 1). Table 2 shows Pt/(Ti + Ga) atomic ratios determined from XPS for the calcined catalysts. Taking into account the Pt content of the catalysts, Pt dispersion values are in good agreement with their relative (Pt/(Ti + Ga))_{XPS}. We have recently shown that for a given Pt content (about 0.5% wt) the preparation method used in this work led to Pt/TiO₂ catalysts with a lower Pt dispersion than the corresponding Pt–Ga/TiO₂ catalyst [19]. In this work we prepared Pt/TiO₂ catalysts with a slightly lower Pt content than that of Pt–Ga/TiO₂ turning out catalysts with similar values of Pt dispersion.

Catalysts were tested at 25 °C in the photocatalytic production of H₂ in liquid phase using 25% v/v ethanol aqueous solutions. Table 2 also shows the rate of H₂ production during the photocatalytic tests. The initial rate of H₂ production was slightly higher for 0.4Pt/TiO₂ and 0.3Pt/TiO₂ than for Pt–Ga/TiO₂. However, after 4 h, 0.4Pt/TiO₂ and 0.3Pt/TiO₂ showed a rate of H₂ production slightly lower than Pt–Ga/TiO₂. Although

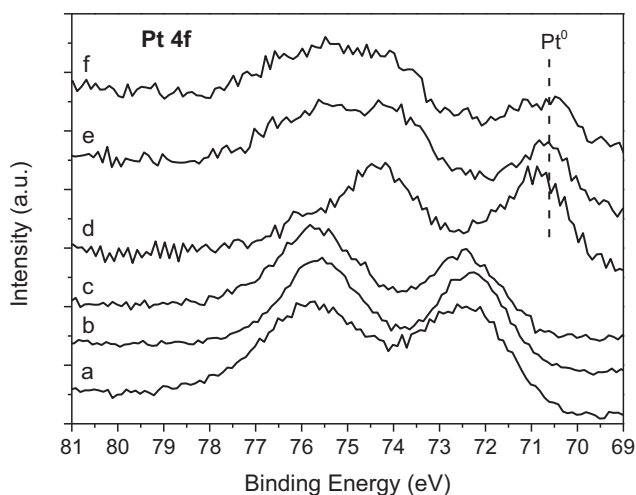


Fig. 1 – XPS spectra corresponding to the Pt 4f core level of catalysts: a) fresh Pt–Ga/TiO₂; b) fresh 0.4Pt/TiO₂; c) fresh 0.3Pt/TiO₂; d) post-reaction Pt–Ga/TiO₂; e) post-reaction 0.4Pt/TiO₂; f) post-reaction 0.3Pt/TiO₂.

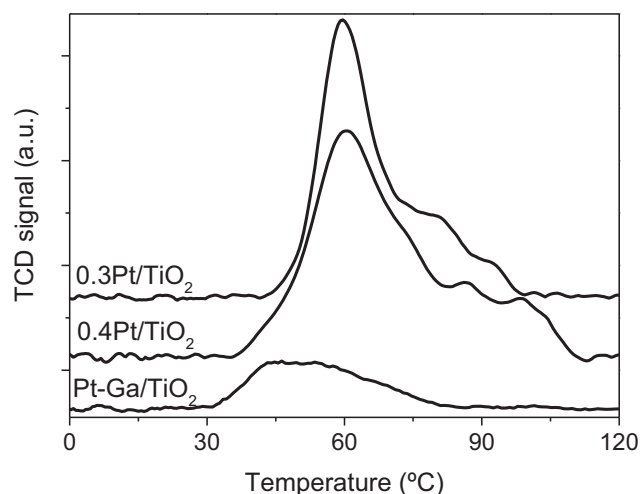


Fig. 2 – Temperature programmed H₂-reduction profiles of catalysts.

Table 2 – Pt/(Ti + Ga) atomic ratio determined by XPS before and after the photocatalytic test and rate of H₂ production during the photocatalytic transformation of 25% (v/v) ethanol_(aq) solutions.

Catalyst	Initial (Pt/(Ti + Ga)) _{XPS}	Final (Pt/(Ti + Ga)) _{XPS}	Initial mmolH ₂ /min	Final (4 h) mmolH ₂ /min
0.3Pt/TiO ₂	0.0111	0.0030 ^a	0.617	0.211
0.4Pt/TiO ₂	0.0080	0.0050 ^a	0.598	0.214
Pt–Ga/TiO ₂	0.0183	0.0152 ^b	0.535	0.224

^a Post-reaction (4 h).^b Post-reaction (24 h) [19].

for all photocatalysts the (Pt/(Ti + Ga))_{XPS} decreased during the test, the diminution was lower for Pt–Ga/TiO₂ than for non-containing Ga catalysts (Table 2).

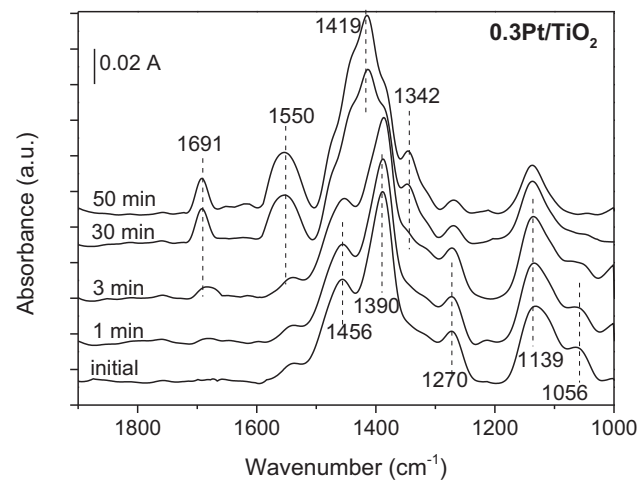
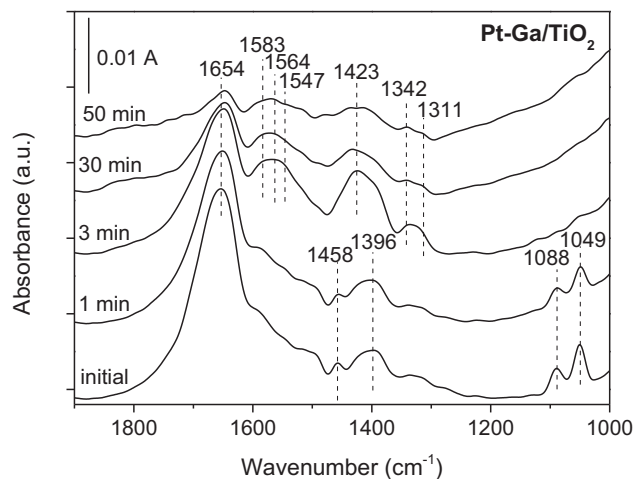
Table 3 compiles the gaseous products determined after 4 h under irradiation. As can be seen, although the main gas-phase product was H₂, lower amounts of CO_x, CH₄, and C₂ hydrocarbons were also formed. Using 0.4Pt/TiO₂ and 0.3Pt/TiO₂ the total amount of H₂ produced was slightly higher than that produced over Pt–Ga/TiO₂ (Table 3). In the liquid phase, besides acetaldehyde, which was the main product, minor amounts of 2,3-butanediol, acetic acid and acetone were found.

According with previous results, under the experimental conditions used, the main reaction is the oxidative dehydrogenation of ethanol to acetaldehyde; the photocatalytic reactions related with the formation of all the other products have been previously discussed [12].

In-situ DRIFTS-MS studies

In-situ DRIFTS-MS studies of the photocatalytic H₂ production from ethanol_(aq) in vapour phase were carried out with Pt–Ga/TiO₂ and 0.3Pt/TiO₂ at 25 °C. Fig. 3 shows the initial spectra in the 1900–1000 cm⁻¹ region after the ethanol/H₂O adsorption and the evolution of the spectra with the irradiation time. For Pt–Ga/TiO₂, the initial spectrum showed clear bands related with the presence of adsorbed bridged ethoxide species at 1088 cm⁻¹ (ν(C–C)) and 1049 cm⁻¹ (ν(C–O)); bands centred at 1458 cm⁻¹ and 1396 cm⁻¹ can be reasonably ascribed to the corresponding ν_{as}(CH₃) and ν_s(CH₃) absorptions [24–27]. The intense and broad band centred at 1654 cm⁻¹ can be related with the ν(C=O) vibration of adsorbed aldehydes such as formaldehyde, acetaldehyde and/or unsaturated aldehydes; weak bands in the region 2725–2830 cm⁻¹ (not shown) could be related with the corresponding ν(C–H) bands [24,28–33]. Moreover, we cannot discard the presence of physisorbed

acetic acid which would show a characteristic ν(C=O) band at 1750 cm⁻¹ [33]. The initial spectrum of Pt–Ga/TiO₂ also showed low intensity bands in the 1600–1300 cm⁻¹ region characteristic of ν_{as}(COO) and ν_s(COO) of different surface carboxylate species. Absorptions at 1583 cm⁻¹ and 1423 cm⁻¹ can be related with ν_{as}(COO) and ν_s(COO) bands of bridged bidentate acetate; the small intensity absorptions at 1547 cm⁻¹ and 1311 cm⁻¹ can be assigned to ν_{as}(COO) and ν_s(COO) bands of adsorbed formate species [34]. During the irradiation, the progressive diminution of the intensity of the

**Fig. 3 – DRIFT spectra in 1900–1000 cm⁻¹ region of Pt–Ga/TiO₂ and 0.3Pt/TiO₂ catalysts after ethanol_(aq) vapour adsorption and evolution with the irradiation time.****Table 3 – Gaseous products obtained during the photocatalytic transformation of 25% (v/v) ethanol_(aq) solutions (t = 4 h).**

Catalyst	Total amount (mmol)					
	H ₂	CO ₂	CH ₄	CO	C ₂ H ₆	C ₂ H ₄
0.3Pt/TiO ₂	85.8	2.2	2.5	1.4	0.5	0.0
0.4Pt/TiO ₂	91.3	2.5	2.9	1.4	0.4	0.0
Pt–Ga/TiO ₂	72.6	1.6	2.1	1.1	0.5	0.1

bands characteristic of ethoxide and aldehyde species took place. The intensity of the bands corresponding to carboxylate (acetate and formate) initially increased under irradiation but then progressively decreased (Fig. 3).

Moreover, during the irradiation $\nu(\text{CO})$ bands related with CO on Pt centres were found. After 3 min of irradiation clear bands at 2086 cm^{-1} and 2022 cm^{-1} related with linearly coordinated CO onto different Pt species appeared (Fig. 4). The intensity of the band at 2086 cm^{-1} decreased and that of the band at a lower wavenumber increased with the irradiation time; after 50 min of irradiation only one band centred at 2040 cm^{-1} and assigned to CO over Pt^0 remained [35–37]. During the irradiation, MS analysis of the products evolved showed the formation of H_2 and other fragments associated to CH_3CHO , CH_3COOH , CH_4 , CO_2 and CO.

A similar DRIFTS-MS study carried out with the $0.3\text{Pt}/\text{TiO}_2$ indicated several differences in the photocatalytic behaviour of $0.3\text{Pt}/\text{TiO}_2$ and $\text{Pt-Ga}/\text{TiO}_2$ (Fig. 3). After adsorption of ethanol_(aq) vapour onto $0.3\text{Pt}/\text{TiO}_2$, wide bands centred at 1139 cm^{-1} and 1056 cm^{-1} were generated, the breadth of these bands could indicate the presence of different surface

ethoxide species bridged and monodentate [26,34]; besides $\nu(\text{C-C})$, $\nu(\text{C-O})$ of monodentate ethoxide species could contribute to the band centred at 1139 cm^{-1} . The corresponding $\nu_{\text{as}}(\text{CH}_3)$ and $\nu_{\text{s}}(\text{CH}_3)$ bands characteristic of adsorbed ethoxide can be seen at 1456 cm^{-1} and 1390 cm^{-1} respectively (Fig. 3). The band at 1270 cm^{-1} could be related with the corresponding $\delta(\text{OH})$ of molecularly adsorbed ethanol whose $\nu(\text{C-C})$ is expected at 1100 cm^{-1} and could contribute to the band centred at 1139 cm^{-1} (initial spectrum of $0.3\text{Pt}/\text{TiO}_2$ in Fig. 3). The intensity of all these bands related with the presence of adsorbed ethanol and ethoxide species decreased with the irradiation time. Meanwhile, under irradiation bands at 1691 cm^{-1} , 1550 cm^{-1} , and a broad band in the $1500\text{--}1300\text{ cm}^{-1}$ region with maxima at 1419 cm^{-1} and 1342 cm^{-1} were progressively formed. The band at 1691 cm^{-1} could be indicative of the presence of acyl species [26,38], and the broad band in the $1500\text{--}1300\text{ cm}^{-1}$ region is related with different carboxylate species as discussed above. Moreover, small bands at 2740 cm^{-1} and 2710 cm^{-1} (zone not shown) could be related with the presence of adsorbed aldehydic species. After 50 min of irradiation, the intensity of the band at 1691 cm^{-1} ($\nu(\text{C=O})$ of acyl species) and that of bands in the region $1600\text{--}1300\text{ cm}^{-1}$ ($\nu(\text{COO})$, $\delta(\text{CH}_3)$, $\delta(\text{CH})$ of acetate/formate species) increased. MS analysis of gases evolved indicated the formation of H_2 and small amounts of CH_4 .

For the $0.3\text{Pt}/\text{TiO}_2$ catalyst, bands in the $\nu(\text{CO})$ zone at 2131 cm^{-1} , 2077 cm^{-1} and 1915 cm^{-1} appeared from the initial stage (Fig. 4). The $\nu(\text{CO})$ band with maximum at 2131 cm^{-1} is related with CO linearly coordinated onto oxidized Pt. After 50 min of irradiation this band disappeared and a main band at 2079 cm^{-1} related with terminal CO coordinated to Pt^0 was clearly visible. This is probably due to the reduction of surface Pt under the photocatalytic process. Clear absorptions below 2000 cm^{-1} are related with the presence of bridged CO. The formation of bridged CO species over $0.3\text{Pt}/\text{TiO}_2$ during the irradiation process contrasts with the behaviour of $\text{Pt-Ga}/\text{TiO}_2$ discussed above (Fig. 4). These results pointed to different characteristics of Pt centres on $\text{Pt-Ga}/\text{TiO}_2$ and $0.3\text{Pt}/\text{TiO}_2$; an effect of Ga in the characteristics of surface Pt centres is shown.

For a better insight in the different transformation of surface species over $\text{Pt-Ga}/\text{TiO}_2$ and $0.3\text{Pt}/\text{TiO}_2$ during irradiation, Fig. 5 illustrates the evolution along the irradiation time of the bands related to the surface ethoxide ($\nu(\text{C-O})$) and carboxylate ($\nu_{\text{as}}(\text{COO})$ and $\nu_{\text{s}}(\text{COO})$) species corresponding to $\text{Pt-Ga}/\text{TiO}_2$ and $0.3\text{Pt}/\text{TiO}_2$.

Fig. 5 clearly shows that in both cases the amount of initial ethoxide species decreased with the irradiation time. However, for $\text{Pt-Ga}/\text{TiO}_2$ the initial high decrease in the amount of ethoxide species is accompanied by a high increase of the surface carboxylate species; after the initial increase, the amount of carboxylate species decreased along time. The degradation of carboxylate species and the diminution of the band at 1654 cm^{-1} characteristic of aldehydic species, is related with the evolution of CH_3CHO , CH_3COOH , CH_4 , CO_2 and CO determined by MS. For $0.3\text{Pt}/\text{TiO}_2$, the amount of surface carboxylate species increased along irradiation time; as stated above, in this case only H_2 and a small amount of CH_4 were detected by MS.

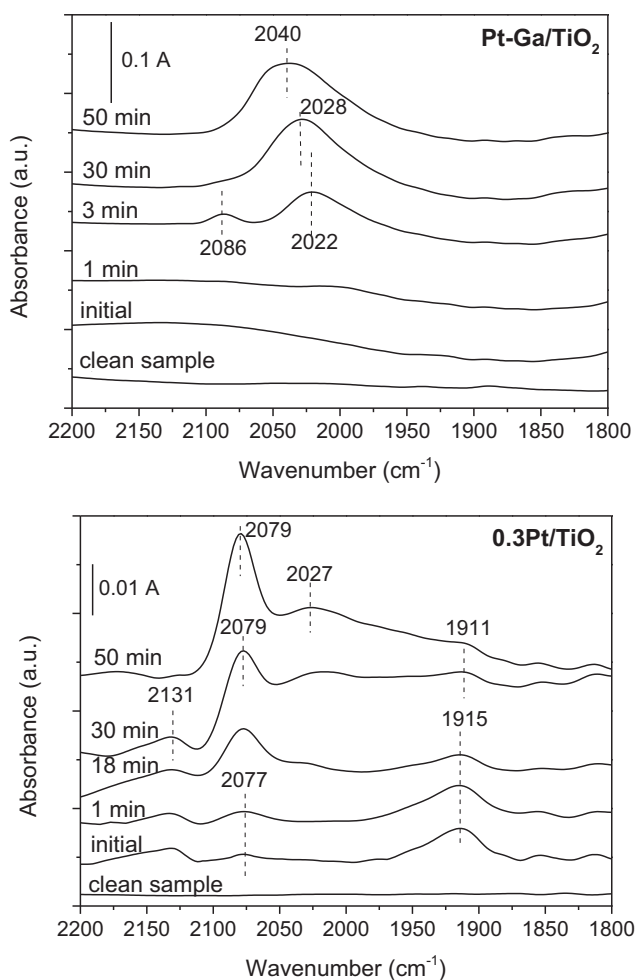


Fig. 4 – DRIFT spectra in $2200\text{--}1800\text{ cm}^{-1}$ region of $\text{Pt-Ga}/\text{TiO}_2$ and $0.3\text{Pt}/\text{TiO}_2$ catalysts after ethanol_(aq) vapour adsorption and evolution with the irradiation time.

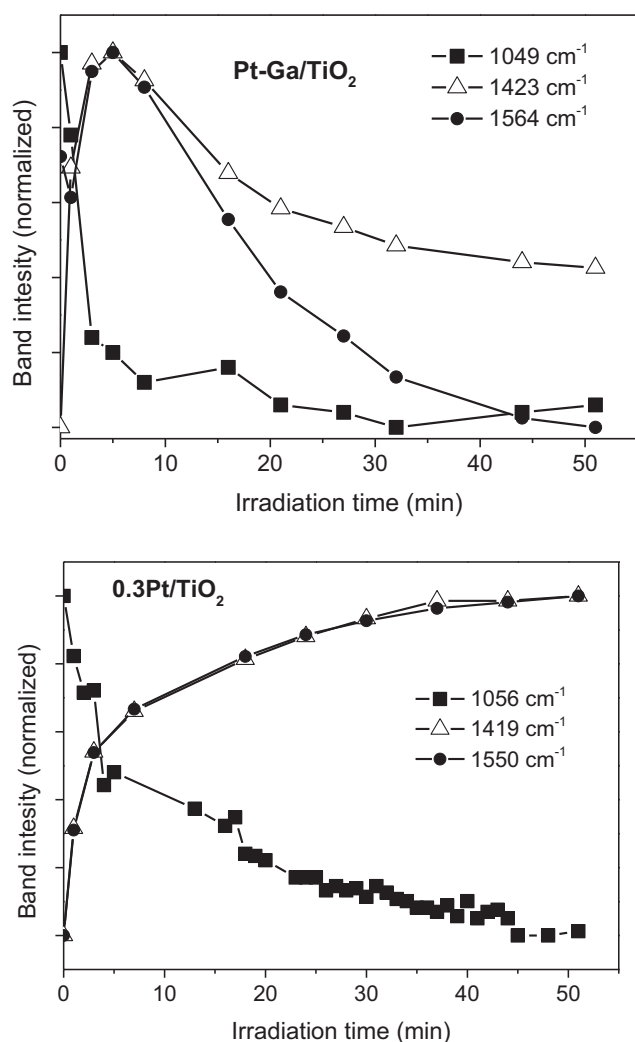


Fig. 5 – Evolution of IR bands corresponding to ethoxide ($\nu(\text{C-O})$) and carboxylate ($\nu_{\text{as}}(\text{COO})$ and $\nu_{\text{s}}(\text{COO})$) species along the irradiation time for Pt–Ga/TiO₂ and 0.3Pt/TiO₂ after ethanol_(aq) vapour adsorption.

Conclusions

Anatase-supported Pt (0.3–0.4% wt) and Pt–Ga (0.5% wt Pt) catalysts with similar Pt dispersion and morphological characteristics were studied in the photocatalytic production of H₂ using ethanol as sacrificial agent. In the photocatalytic test in liquid phase (4 h), H₂ and acetaldehyde were the main products found. The total amount of H₂ produced and the initial rate of H₂ production were slightly higher for Pt/TiO₂ than for Pt–Ga/TiO₂. However, Pt/TiO₂ showed slightly lower final rate of H₂ production than Pt–Ga/TiO₂; for Pt–Ga/TiO₂, the (Pt/(Ti + Ga))_{XPS} diminution during the test was lower than for Pt/TiO₂ catalysts.

In situ DRIFTS-MS studies carried out with Pt–Ga/TiO₂ and 0.3Pt/TiO₂ evidenced the formation of aldehydic and carboxylate surface species after vapour adsorption of ethanol_(aq). The photocatalytic transformation of these surface species

was more effective over Pt–Ga/TiO₂ than over 0.3Pt/TiO₂. For Pt/TiO₂, the amount of surface carboxylate species increased along the irradiation time and only H₂ and a small amount of CH₄ were evolved. For Pt–Ga/TiO₂, a clear degradation of carboxylate species during the irradiation was found, and besides H₂ and CH₄, CH₃CHO, CH₃COOH, CO₂ and CO were detected in the gas phase. The $\nu(\text{CO})$ bands risen during the DRIFTS-MS experiments pointed to an effect of Ga, likely a dilution effect on surface Pt species, for the Pt–Ga/TiO₂ catalyst.

Acknowledgements

The authors are grateful to the projects MAT2014-52416-P and MAT2017-87500-P for financial support. A. C. Sola also thanks the IREC for his PhD grant 06/10.

REFERENCES

- [1] Sakata T, Kawai T. Heterogeneous photocatalytic production of hydrogen and methane from ethanol and water. *Chem Phys Lett* 1981;80:341–4.
- [2] Nada AA, Barakat MH, Hamed HA, Mohamed NR, Veziroglu TN. Studies on the photocatalytic hydrogen production using suspended modified TiO₂ photocatalysts. *Int J Hydrogen Energy* 2005;30:687–91.
- [3] Strataki N, Bekiari V, Kondarides DI, Lianos P. Hydrogen production by photocatalytic alcohol reforming employing highly efficient nanocrystalline titania films. *Appl Catal B* 2007;77:184–9.
- [4] Strataki N, Antoniadou M, Dracopoulos V, Lianos P. Visible-light photocatalytic hydrogen production from ethanol–water mixtures using a Pt–CdS–TiO₂ photocatalyst. *Catal Today* 2010;151:53–7.
- [5] Languer MP, Scheffer FR, Feil AF, Baptista DL, Migowski P, Machado GJ, et al. Photo-induced reforming of alcohols with improved hydrogen apparent quantum yield on TiO₂ nanotubes loaded with ultra-small Pt nanoparticles. *Int J Hydrogen Energy* 2013;38:14440–50.
- [6] Puskelova J, Baia L, Vulpoi A, Baia M, Antoniadou M, Dracopoulos V, et al. Photocatalytic hydrogen production using TiO₂-Pt aerogels. *Chem Eng J* 2014;242:96–101.
- [7] Beltram A, Romero-Ocana I, Jaen JJD, Montini T, Fornasiero P. Photocatalytic valorization of ethanol and glycerol over TiO₂ polymorphs for sustainable hydrogen production. *Appl Catal A* 2016;518:167–75.
- [8] López CR, Melián EP, Ortega Méndez JA, Santiago DE, Doña Rodríguez JM, González Díaz O. Comparative study of alcohols as sacrificial agents in H₂ production by heterogeneous photocatalysis using Pt/TiO₂ catalysts. *J Photochem Photobiol A Chem* 2015;312:45–54.
- [9] Bowker M, Bahruji H, Kennedy J, Jones W, Hartley G, Morton C. The photocatalytic window: photo-reforming of organics and water splitting for sustainable hydrogen production. *Catal Lett* 2015;145:214–9.
- [10] Zakiya HN, Al-Azri Chen WT, Chan A, Jovic V, Ina T, Idriss H, et al. The roles of metal co-catalysts and reaction media in photocatalytic hydrogen production: performance evaluation of M/TiO₂ photocatalysts (M=Pd, Pt, Au) in different alcohol-water mixtures. *J Catal* 2015;329:355–67.
- [11] Shimura K, Yoshida H. Heterogeneous photocatalytic hydrogen production from water and biomass derivatives. *Energy Environ Sci* 2011;4:2467–81.

- [12] Sola AC, Homs N, Ramírez de la Piscina P. Photocatalytic H₂ production from ethanol_(aq) solutions: the effect of intermediate products. *Int J Hydrogen Energy* 2016;41:19629–36.
- [13] Bamwenda GR, Tsubota S, Nakamura T, Haruta M. Photoassisted hydrogen production from a water-ethanol solution: a comparison of activities of Au/TiO₂ and Pt/TiO₂. *J Photochem Photobiol A Chem* 1995;89:177–89.
- [14] Yang YZ, Chang CH, Idriss H. Photocatalytic production of hydrogen from ethanol over M/TiO₂ catalysts (M = Pd, Pt or Rh). *Appl Catal B Environ* 2006;67:217–22.
- [15] Lu H, Zhao J, Li L, Gong L, Zheng J, Zhang L, et al. Selective oxidation of sacrificial ethanol over TiO₂-based photocatalysts during water splitting. *Energy Environ Sci* 2011;4:3384–8.
- [16] Gong D, Subramaniam VP, Highfield JG, Tang Y, Lai Y, Chen Z. In-situ mechanistic investigation at the liquid/solid interface by ATR-FTIR: ethanol photo-oxidation over pristine and platinumized TiO₂ (P25). *ACS Catal* 2011;1:864–71.
- [17] Majrik K, Tálas E, Pászti Z, Sajó I, Mihály J, Korecz L, et al. Enhanced activity of sol-gel prepared SnO_x-TiO₂ in photoatalytic methanol reforming. *Appl Catal A Gen* 2013;466:169–78.
- [18] Leung DYC, Fu X, Wang C, Ni M, Leung MKH, Wang X, et al. Hydrogen production over titania-based photocatalysts. *ChemSusChem* 2010;3:681–94.
- [19] Sola AC, Gösler MB, Ramírez de la Piscina P, Homs N. Promoter effect of Ga in Pt/Ga-TiO₂ catalysts for the photo-production of H₂ from aqueous solutions of ethanol. *Catal Today* 2017;287:85–90.
- [20] Reyes-Coronado D, Rodríguez-Gattorno G, Espinosa-Pesqueira ME, Cab C, de Coss R, Oskam G. Phase-pure TiO₂ nanoparticles: anatase, brookite and rutile. *Nanotechnology* 2008;19:145605.
- [21] Zhang J, Li M, Feng Z, Chen J, Li C. UV Raman spectroscopic study on TiO₂. I. Phase transformation at the surface and in the bulk. *J Phys Chem B* 2006;110:927–35.
- [22] Jensen H, Soloviev A, Li Z, Søggaard EG. XPS and FTIR investigation of the surface properties of different prepared titania nano-powders. *Appl Surf Sci* 2005;246:239–49. <https://doi.org/10.1016/j.apsusc.2004.11.015>.
- [23] Ono LK, Croy JR, Heinrich H, Cuenya BR. Oxygen chemisorption, formation, and thermal stability of Pt oxides on Pt nanoparticles supported on SiO₂/Si (001): size effects. *J Phys Chem C* 2011;115:16856–66.
- [24] Nadeem AM, Waterhouse GIN, Idriss H. The reactions of ethanol on TiO₂ and Au/TiO₂ anatase catalysts. *Catal Today* 2012;182:16–24.
- [25] Carvalho DL, Borges LEP, Appel LG, Ramírez de la Piscina P, Homs N. In situ infrared spectroscopic study of the reaction pathway of the direct synthesis of n-butanol from ethanol over MgAl mixed-oxide catalysts. *Catal Today* 2013;213:115–21.
- [26] Llorca J, Homs N, Ramírez de la Piscina P. In situ DRIFT-mass spectrometry study of the ethanol steam-reforming reaction over carbonyl-derived Co/ZnO catalysts. *J Catal* 2004;227:556–60.
- [27] Yee A, Morrison SJ, Idriss H. A study of the reactions of ethanol on CeO₂ and Pd/CeO₂ by steady state reactions, temperature programmed desorption, and in situ FT-IR. *J Catal* 1999;186:279–95.
- [28] Sola AC, Garzón Sousa J, Araña O, González Díaz JM, Doña Rodríguez, Ramírez de la Piscina P, et al. Differences in the vapour phase photocatalytic degradation of ammonia and ethanol in the presence of water as a function of TiO₂ characteristics and the presence of O₂. *Catal Today* 2016;266:53–6.
- [29] Singh M, Zhou N, Paul DK, Klabunde KJ. IR spectral evidence of aldol condensation: acetaldehyde adsorption over TiO₂ surface. *J Catal* 2008;260:371–9.
- [30] De Jesús JC, Zaera F. Adsorption and thermal chemistry of acrolein and crotonaldehyde on Pt(111) surfaces. *Surf Sci* 1999;430:99–115.
- [31] Carriazo D, Martín C, Rives V. An FT-IR study of the adsorption of isopropanol on calcined layered double hydroxides containing isopolymolybdate. *Catal Today* 2007;126:153–61.
- [32] Ordonsky VV, Sushkevich VL, Ivanova II. Study of acetaldehyde condensation chemistry over magnesia and zirconia supported on silica. *J Mol Catal A Chem* 2010;333:85–93.
- [33] Liao L-F, Lien C-F, Lin J-L. FTIR study of adsorption and photoreactions of acetic acid on TiO₂. *Phys Chem Chem Phys* 2001;3:3831–7.
- [34] Coronado JM, Kataoka S, Tejedor-Tejedor I, Anderson MA. Dynamic phenomena during the photocatalytic oxidation of ethanol and acetone over nanocrystalline TiO₂: simultaneous FTIR analysis of gas and surface species. *J Catal* 2003;219:219–30.
- [35] Coloma F, Coronado JM, Rochester CH, Anderson JA. Infrared study of crotonaldehyde and CO adsorption on a Pt/TiO₂ catalyst. *Catal Lett* 1998;51:155–62.
- [36] Silvestre-Albero J, Sepúlveda-Escribano A, Rodríguez-Reinoso F, Anderson JA. Influence of Zn on the characteristics and catalytic behavior of TiO₂-supported Pt catalysts. *J Catal* 2004;223:179–90.
- [37] Ruiz-Martínez J, Sepúlveda-Escribano A, Anderson JA, Rodríguez-Reinoso F. Spectroscopic and microcalorimetric study of a TiO₂-supported platinum catalyst. *Phys Chem Chem Phys* 2009;11:917–20.
- [38] Rachmady W, Vannice MA. Acetic acid reduction by H₂ over supported Pt Catalysts: a DRIFTS and TPD/TPR study. *J Catal* 2002;207:317–30.